# Nonasymptotic E-Optimal Design of Experiments for System Identification Using Sign-Perturbed Sums ⋆

**Masanori Oshima** * **Sanghong Kim** ** **Yuri A. W. Shardt** *** **Ken-Ichiro Sotowa** *

* *Department of Chemical Engineering, Kyoto University, Kyoto 615-8510, Japan (e-mail: masanori.9221.sskt@outlook.jp, sotowa@cheme.kyoto-u.ac.jp).*
** *Department of Applied Physics and Chemical Engineering, Tokyo University of Agriculture and Technology, Tokyo 184-8588, Japan, (e-mail: sanghong@go.tuat.ac.jp)*
*** *Department of Automation Engineering, Technical University of Ilmenau, Ilmenau D-98684, Germany, (e-mail: yuri.shardt@tu-ilmenau.de)*

**Abstract:** Design of experiments (DoE) helps us to obtain an accurate model using system identification. However, most DoE methods rely on asymptotic theory and assume availability of infinite data samples. To overcome this problem, Oshima et al. (2024) proposed a DoE method that evaluates the data quality using the volume of the nonasymptotic confidence region (CR) calculated using sign-perturbed sums (SPS) proposed by Csáji and Weyer (2015). This paper modifies the DoE objective function defined by Oshima et al. (2024) to derive a nonasymptotic counterpart of the E-optimal DoE, which minimizes the length of the longest axis of the asymptotic confidence ellipsoid. The proposed data-quality index is defined by the maximum distance from the center point to the points on the boundaries of the nonasymptotic CR. Moreover, a necessary condition for the points in the parameter space to be on the boundaries of the nonasymptotic CR obtained using the SPS method is theoretically derived. Based on this condition, an algorithm to calculate the maximum distance is proposed. The proposed nonasymptotic E-optimal DoE was validated in a numerical case study, where a 2-input, 3-output ARX system was targeted. As a result, it was shown that the nonasymptotic E-optimal DoE provides a more accurate model compared with the asymptotic E-optimal DoE.

*Keywords:* system identification, design of experiments, finite-sample data, nonasymptotic confidence region, E-optimal design

## 1. INTRODUCTION

In process systems, dynamic models are often built using system identification, where the model parameters are estimated using only the time-series data of the input and output variables. This estimated model is used in model-based control, such as model predictive control (MPC) (Morari and H. Lee, 1999), to realize advanced operations, such as minimizing energy consumption while satisfying the requirement for product quality. Using an accurate model in model-based control is essential to obtaining optimal results from such advanced operations.

The accuracy of the model parameters estimated using system identification depends not only on the identification method but also on how the data for identification is collected. Hence, it is crucial to determine the experimental condition for data collection, such as the amplitudes and frequencies of the external input signals, so that useful data for system identification can be obtained.

Design of experiments (DoE) for identification (Goodwin, 1977) is helpful for this objective. DoE determines the experimental conditions by maximizing a data-quality index, which is defined based on the uncertainty of the model parameters.

The data-quality indices of the classical DoE methods, which are elaborated by Goodwin (1977) and Shardt (2022), use the asymptotic confidence region (CR) as an uncertainty of the model parameters. Let the confidence probability be $p$, then the asymptotic CR includes the true parameter vector with probability $p$ if the least-squares estimates of the model parameters follow a Gaussian distribution (Ljung, 1998). This holds either when the noise innovations of the target system follow a Gaussian distribution or when the number of samples is so large that the central limit theorem approximately holds. However, in the actual situation of the process systems, the noise innovations do not always follow a Gaussian distribution,

⋆ This work was supported by JSPS KAKENHI, Grant Numbers JP22K04816 and JP24KJ1369.

and the number of available samples is often limited. Hence, the suggestions by the classical DoE methods may not suit many practical situations. Therefore, a data-quality index based on a nonasymptotic uncertainty that is accurate even when applied to such situations is desirable.

The sign-perturbed-sums (SPS) method, which was developed by Csáji et al. (2012, 2015), provides an exact nonasymptotic CR of the process parameters. Moreover, the SPS method does not rely on the assumption that restricts the distribution of the noise innovation to a particular type, such as a Gaussian or a uniform distribution. Instead, it only assumes that the noise innovation has a symmetric distribution. Hence, the SPS method is applied to many practical situations without violating the assumption.

As well, the SPS method have been extended to various types of systems. Csáji et al. (2012) proposed the SPS algorithm for general single-input, single-output (SISO) linear systems. Csáji and Weyer (2015) extended the SPS algorithm to SISO closed-loop systems with linear processes. Extensions to multivariate systems with or without closed loops were also proposed by Szentpéteri and Csáji (2023) and Oshima et al. (2023).

The SPS method has been used for DoE in a few previous papers (Kolumbán and Csáji, 2018; Oshima et al., 2024). Kolumbán and Csáji (2018) minimized the expected value of the volume of the nonasymptotic CR obtained using the SPS method. However, their DoE problem restricts the target systems to SISO finite-impulse-response (FIR) systems, so that it can be solved offline. Hence, it cannot be applied to more complicated systems, such as multi-input, multi-output systems with regressors comprised of sequences of both the past inputs and outputs. Oshima et al. (2024) solved this problem by defining the data-quality index based on the volume of the nonasymptotic CR for multivariate autoregressive exogenous input (ARX) systems. Furthermore, an approach that iteratively performs a data-collection experiment using Bayesian optimization (BO) (Shahriari et al., 2016) was introduced to solve the optimization problem of DoE including an objective function dependent on the outcome of the experiment.

However, all of these use the data-quality index based on the CR volume, that is, they are nonasymptotic counterparts of the D-optimal design. There is no nonasymptotic DoE method comparable with the E-optimal design, which quantifies the uncertainty of the model parameters by the longest axis of the asymptotic CR, which is an ellipsoid. Thus, this paper proposes a nonasymptotic E-optimal DoE method based on the nonasymptotic CR obtained using the SPS method.

## 2. NOMENCLATURE

Vectors and matrices are written in lowercase and uppercase boldface, respectively, in this paper. Sets are written in uppercase blackboard font. In addition, the following symbols are used:

(1) $\mathbb{Z}$: the set of integers.
(2) $\mathbb{Z}_{i\leq,\leq j} = \mathbb{Z} \cap \{x \in \mathbb{R} \mid i \leq x \leq j\}$ for $i, j \in \mathbb{Z}$ such that (s.t.) $i < j$.
(3) $\mathbb{Z}_{i\leq} = \mathbb{Z} \cap \{x \in \mathbb{R} \mid x \geq i\}$ for $i \in \mathbb{Z}$.
(4) $[a, b]^i = \{[x_1, \cdots, x_i]^\top \in \mathbb{R}^i \mid a \leq x_{i'} \leq b, \forall i' \in \mathbb{Z}_{1\leq,\leq i}\}$ for $a, b \in \mathbb{R}$ and $i \in \mathbb{Z}_{2\leq}$
(5) $\varnothing$: the empty set.

## 3. BACKGROUND

### 3.1 Target system

The target system is an $M$-input, $N$-output ARX system. The outputs, inputs, and noise innovations at time index $t$ are $\boldsymbol{y}_t = [y_{1,t}, \cdots, y_{N,t}]^\top$, $\boldsymbol{u}_t = [u_{1,t}, \cdots, u_{M,t}]^\top$, and $\boldsymbol{e}_t = [e_{1,t}, \cdots, e_{N,t}]^\top$. Thus, the process of interest is

$$\boldsymbol{y}_t = \sum_{k=1}^{K} \boldsymbol{A}_k \boldsymbol{y}_{t-k} + \sum_{l=1}^{L} \boldsymbol{B}_l \boldsymbol{u}_{t-l} + \boldsymbol{e}_t, \tag{1}$$

where $K$ and $L$ are the maximum time delays of the outputs and inputs of the process, $\boldsymbol{A}_k \in \mathbb{R}^{N\times N}$ and $\boldsymbol{B}_l \in \mathbb{R}^{N\times M}$ are the process parameters.

Let $\underline{\tau}_{n,m} \in \mathbb{Z}_{1\leq,\leq L}$ and $\overline{\tau}_{n,m} \in \mathbb{Z}_{\underline{\tau}_{n,m}\leq,\leq L}$ be respectively the minimum and maximum time delays between $y_{n,t}$ and $u_{m,t}$. Then, the number $d$ of the process parameters is

$$d = KN^2 + \sum_{n=1}^{N}\sum_{m=1}^{M} (\overline{\tau}_{n,m} - \underline{\tau}_{n,m} + 1), \tag{2}$$

and Eq. (1) is transformed into

$$\boldsymbol{y}_t = \boldsymbol{\Phi}_t^\top \boldsymbol{\theta}^* + \boldsymbol{e}_t, \tag{3}$$

$$\boldsymbol{\Phi}_t = \begin{bmatrix} \boldsymbol{\phi}_{1,t} & & 0 \\ & \ddots & \\ 0 & & \boldsymbol{\phi}_{N,t} \end{bmatrix}, \tag{4}$$

$$\begin{aligned} \boldsymbol{\phi}_{n,t} = [&-y_{1,t-1}, \cdots, -y_{1,t-K}, \cdots, \\ &-y_{N,t-1}, \cdots, -y_{N,t-K}, \\ &u_{1,t-\underline{\tau}_{n,1}}, \cdots, u_{1,t-\overline{\tau}_{n,1}}, \cdots, \\ &u_{M,t-\underline{\tau}_{n,M}}, \cdots, u_{M,t-\overline{\tau}_{n,M}}]^\top, \end{aligned} \tag{5}$$

where $\boldsymbol{\theta}^* \in \mathbb{R}^d$ and $\boldsymbol{\Phi}_t \in \mathbb{R}^{d\times N}$ are the true parameter vector and the regressor matrix, respectively.

$T$ samples of $\boldsymbol{y}_t$ and $\boldsymbol{u}_t$ are collected in the process of Eq. (1) or Eqs. (3) to (5), based on which $\boldsymbol{\theta}^*$ is estimated using least-square estimation. The least-squares estimates of $\boldsymbol{\theta}^*$ are denoted by $\boldsymbol{\theta}_{\mathrm{LS}}$.

### 3.2 Sign-perturbed sums

The SPS method (Csáji et al., 2012; Csáji and Weyer, 2015; Csáji et al., 2015; Szentpéteri and Csáji, 2023; Oshima et al., 2023) examines as many parameter vectors as possible using the following procedure for finding the set of the points included in the CR. The SPS method generates $R$ sets of time series of noise innovations by randomly perturbing the signs of the noise innovation estimated using a parameter vector $\boldsymbol{\theta}$ of interest and the original input-output data obtained in the target system. Then, $R$ sets of input-output data are generated from the simulation of the model with $\boldsymbol{\theta}$ that is driven by the generated noise innovations. The generated data sets are compared with the original data set in the Euclidean norm of a vector index, called the reference sum for the original data set and sign-perturbed sums for the generated data sets. If the norm of reference sum is smaller than the $\tilde{R}$-th

largest norm of sign-perturbed sum, then the SPS method determines $\boldsymbol{\theta}$ is in the target region, that is,

$$\boldsymbol{\theta} \in \mathbb{D}_{\mathrm{SPS}} \text{ if and only if } \mathrm{Rank}(\boldsymbol{\theta}) \leq R - \tilde{R} \tag{6}$$

where $\mathbb{D}_{\mathrm{SPS}}$ is the CR obtained using the SPS method, and $\mathrm{Rank}(\boldsymbol{\theta})$ expresses the rank of the reference sum in the ranking of the norms of reference sum and sign-perturbed sums from the smallest to the largest (see Appendix. A). $R \in \mathbb{Z}_{1\leq}$ and $\tilde{R} \in \mathbb{Z}_{1\leq,\leq R-1}$ are the hyperparameters of the SPS method that determine the confidence probability $p_{\mathrm{SPS}}$ of $\mathbb{D}_{\mathrm{SPS}}$ as

$$p_{\mathrm{SPS}} = 1 - \frac{\tilde{R}}{R}. \tag{7}$$

Previous papers on the SPS method have mathematically proved that the actual confidence probability of $\mathbb{D}_{\mathrm{SPS}}$ is exactly equal to $p_{\mathrm{SPS}}$, which makes the SPS method a reliable tool to evaluate the nonasymptotic CR. Furthermore, the exactness of the SPS method does not rely on the values of $R$ and $\tilde{R}$. In the case of multivariate ARX systems, the following assumptions are made for the proof (Oshima et al., 2023):

- A.1 $\{e_{n,t}\}$ are independent, and the probability density function (PDF) of each $e_{n,t}$ is symmetric about 0.
- A.2 The other external signals are independent of $\{e_{n,t}\}$.
- A.3 The model has the same structure as the system given by Eqs. (3) to (5).

Note that A.1 simply requires the PDF of the noise innovation to be a symmetric function and does not require a specific type of PDF such as a Gaussian distribution. This allows us to apply the SPS method to practical cases where the PDF of the noise innovation is not accurately known.

## 4. METHOD

This section describes both asymptotic and nonasymptotic DoE methods. Both of the DoE methods commonly optimize the design variables $\boldsymbol{\chi}$, which corresponds to the properties of the external input signals, such as frequencies. On the other hand, the objective functions of the asymptotic and nonasymptotic DoE methods are different, which are described in the sections below.

### *4.1 Asymptotic E-optimal objective function*

Asymptotic E-optimal DoE maximizes the minimum eigenvalue of the Fisher information matrix $\boldsymbol{F}$, that is, the asymptotic E-optimal objective function $J_{\mathrm{A}}$ is

$$J_{\mathrm{A}} = \ln(\lambda_{\min}(\boldsymbol{F})),\ \boldsymbol{F} = \frac{1}{T}\sum_{t=1}^{T} \boldsymbol{\Phi}_t \boldsymbol{\Phi}_t^{\top}, \tag{8}$$

where $\lambda_{\min}(\cdot)$ is a function that returns the minimum eigenvalue of the input matrix. Moreover, the inverse of the minimum eigenvalue of $\boldsymbol{F}$ corresponds to the length $l_{\mathrm{A}}$ of the longest axis of the asymptotic CR $\mathbb{D}_{\mathrm{A}}$ (Franceschini and Macchietto, 2008), which is a $d$-dimensional ellipsoid with center $\boldsymbol{\theta}_{\mathrm{LS}}$ (Ljung, 1998). Hence, $J_{\mathrm{A}}$ is expressed using $l_{\mathrm{A}}$ as follows:

$$J_{\mathrm{A}} = \ln((l_{\mathrm{A}}T)^{-1}) + C, \tag{9}$$

where $C$ is a constant that depends on the confidence probability and the variance of $\boldsymbol{e}_t$.

### *4.2 Nonasymptotic E-optimal objective function*

Based on Eq. (9), the maximized objective function $J_{\mathrm{N}}$ of the nonasymptotic E-optimal DoE is defined using a representative length $l_{\mathrm{SPS}}$ of $\mathbb{D}_{\mathrm{SPS}}$ as follows:

$$J_{\mathrm{N}} = \ln((l_{\mathrm{SPS}}T)^{-1}). \tag{10}$$

In Eq. (10), the ratio $\tilde{R}/R$ of the hyperparameters is determined such that $1 - \tilde{R}/R$ will be the probability of interest. The magnitudes of $R$ and $\tilde{R}$ should be as large as the computational resources allow. This is because the stochastic fluctuation of the CR boundary caused by using random signs is alleviated by increasing $R$ and $\tilde{R}$.

Since $\mathbb{D}_{\mathrm{SPS}}$ is not necessarily an ellipsoid, the length of the longest axis is not defined in $\mathbb{D}_{\mathrm{SPS}}$. On the other hand, the length of the longest axis of the asymptotic confidence ellipsoid can be regarded as the maximum value of the distances between $\boldsymbol{\theta}_{\mathrm{LS}}$ and any points in $\mathbb{D}_{\mathrm{SPS}}$. Based on this notion, let $l_{\mathrm{SPS}}$ be defined as

$$l_{\mathrm{SPS}} = \max_{\boldsymbol{\theta} \in \mathbb{D}_{\mathrm{SPS}}} \|\boldsymbol{\theta} - \boldsymbol{\theta}_{\mathrm{LS}}\|. \tag{11}$$

### *4.3 How to calculate $l_{\mathrm{SPS}}$*

From the definition of the SPS algorithm, the least-squares estimates are included in $\mathbb{D}_{\mathrm{SPS}}$. Hence, $\|\boldsymbol{\theta} - \boldsymbol{\theta}_{\mathrm{LS}}\|$ takes the maximum value for $\boldsymbol{\theta} \in \mathbb{D}_{\mathrm{SPS}}$ when $\boldsymbol{\theta}$ is on the boundaries of $\mathbb{D}_{\mathrm{SPS}}$. Therefore, let $\mathbb{B}_{\mathrm{SPS}}$ be the boundaries of $\mathbb{D}_{\mathrm{SPS}}$. Then, Eq. (11) is

$$l_{\mathrm{SPS}} = \max_{\boldsymbol{\theta} \in \mathbb{B}_{\mathrm{SPS}}} \|\boldsymbol{\theta} - \boldsymbol{\theta}_{\mathrm{LS}}\|. \tag{12}$$

From Eq. (12), it is necessary to find the points on the boundaries of $\mathbb{D}_{\mathrm{SPS}}$. Theorem 1 can be used for this.

*Theorem 1.* Let $\mathbb{D}_{\mathrm{SPS}}$ be a bounded region. Then, the rank of the SPS method satisfies,

$$\mathrm{Rank}(\boldsymbol{\theta}) = R - \tilde{R}\ \ , \forall \boldsymbol{\theta} \in \mathbb{B}_{\mathrm{SPS}}. \tag{13}$$

□

**Proof.** See Appendix B.

Theorem 1 implies that $\mathrm{Rank}(\cdot)$ always returns $R - \tilde{R}$ for the points in $\mathbb{B}_{\mathrm{SPS}}$. Hence, we can relax Eq. (12) into

$$l_{\mathrm{SPS}} = \max_{\mathrm{Rank}(\boldsymbol{\theta}) = R - \tilde{R}} \|\boldsymbol{\theta} - \boldsymbol{\theta}_{\mathrm{LS}}\|. \tag{14}$$

Based on Eq. (14), the algorithm to calculate $l_{\mathrm{SPS}}$ is shown as Algorithm 1. The loop from lines 2 to 8 finds a point in $\mathbb{D}_{\mathrm{SPS}}$ as far from $\boldsymbol{\theta}_{\mathrm{LS}}$ as possible using quasi-random sampling based on a Sobol series (Kocis and Whiten, 1997). The value of $\delta l > 0$ used in this loop is determined to be sufficiently small so that $\mathbb{S}_{\mathrm{SPS}}$ will not be an empty set at $l = 0$. Lines 9 to 12 guarantee that $\boldsymbol{\theta}_{\max}$ satisfies the boundary condition in Theorem 1. Moreover, line 10 is achieved by applying the bisection method to $g(\cdot) = \mathrm{Rank}(\texttt{halfline}(\cdot, \boldsymbol{\theta}_{\max})) - (R - \tilde{R})$ between $\kappa = 1$ and sufficiently large $\kappa$ s.t. $g(\kappa) > 0$.

### *4.4 Solving the optimization problem of DoE*

Since $J_{\mathrm{N}}$ and $J_{\mathrm{A}}$ in the case of the ARX systems depend on the outcome of the data-acquisition experiment, they are maximized by the iterative experiment approach using BO proposed by Oshima et al. (2024). Let the objective

**Algorithm 1** Calculation of $l_{\mathrm{SPS}}$

Initialize $l = 0$.
**repeat**
  Let $\mathbb{S}_{\mathrm{sobol}}(l+\delta l)$ be a Sobol series in $\{\boldsymbol{x} + \boldsymbol{\theta}_{\mathrm{LS}} \mid \forall \boldsymbol{x} \in [-(l+\delta l), l+\delta l]^d\}$.
  $\mathbb{D}_{\mathrm{shell}} \leftarrow \{\boldsymbol{\theta} \in \mathbb{R}^d \mid l \le \|\boldsymbol{\theta} - \boldsymbol{\theta}_{\mathrm{LS}}\| \le l + \delta l\}$
  $\mathbb{S}_{\mathrm{shell}} \leftarrow \{\boldsymbol{\theta}_i \in \mathbb{D}_{\mathrm{shell}} \cap \mathbb{S}_{\mathrm{sobol}}(l+\delta l)\}_{i=1}^{I}$
  $\mathbb{S}_{\mathrm{SPS}} \leftarrow \{\boldsymbol{\theta} \in \mathbb{S}_{\mathrm{shell}} \mid \mathrm{Rank}(\boldsymbol{\theta}) \le R - \tilde{R}\}$
  $\boldsymbol{\theta}_{\max} \leftarrow \arg\max_{\boldsymbol{\theta} \in \mathbb{S}_{\mathrm{SPS}}} \|\boldsymbol{\theta} - \boldsymbol{\theta}_{\mathrm{LS}}\|$, $l \leftarrow \|\boldsymbol{\theta}_{\max} - \boldsymbol{\theta}_{\mathrm{LS}}\|$
**until** $\mathbb{S}_{\mathrm{SPS}} = \varnothing$
**if** $\mathrm{Rank}(\boldsymbol{\theta}_{\max}) < R - \tilde{R}$ **then**
  $\kappa_{\max} \leftarrow \kappa$ s.t. $\mathrm{Rank}(\texttt{halfline}(\kappa, \boldsymbol{\theta}_{\max})) = R - \tilde{R}$
  $\boldsymbol{\theta}_{\max} \leftarrow \texttt{halfline}(\kappa_{\max}, \boldsymbol{\theta}_{\max})$
**end if**
**return** $l_{\mathrm{SPS}} = \|\boldsymbol{\theta}_{\max} - \boldsymbol{\theta}_{\mathrm{LS}}\|$
**function** $\texttt{halfline}(\kappa \in (0,\infty), \boldsymbol{\theta}_{\max} \in \mathbb{R}^d)$
  **return** $\kappa(\boldsymbol{\theta}_{\max} - \boldsymbol{\theta}_{\mathrm{LS}}) + \boldsymbol{\theta}_{\mathrm{LS}}$
**end function**

function and the design variables of the DoE be $J$ and $\boldsymbol{\chi}$, respectively. In addition, let the values of $J$ and $\boldsymbol{\chi}$ at the $i_{\mathrm{BO}}$-th experiment be $J_{i_{\mathrm{BO}}}$ and $\boldsymbol{\chi}_{i_{\mathrm{BO}}}$, respectively. Then, after performing $N_{\mathrm{BO,init}}$ experiments to obtain the initial dataset $\{J_i, \boldsymbol{\chi}_i\}_{i=1}^{N_{\mathrm{BO,init}}}$, the following procedure is iterated from $i_{\mathrm{BO}} = N_{\mathrm{BO,init}}$ to $i_{\mathrm{BO}} = N_{\mathrm{BO}} - 1$:

B.1 Based on the dataset $\{J_i, \boldsymbol{\chi}_i\}_{i=1}^{i_{\mathrm{BO}}}$, the next point of $\boldsymbol{\chi}_{i_{\mathrm{BO}}+1}$ is determined according to the BO algorithm.
B.2 A data-acquisition experiment is performed for $T$ samples at the experimental condition determined by $\boldsymbol{\chi}_{i_{\mathrm{BO}}+1}$.
B.3 Based on the data, the objective function value $J_{i_{\mathrm{BO}}+1}$ is evaluated, and $i_{\mathrm{BO}}$ is updated to $i_{\mathrm{BO}} + 1$.

$N_{\mathrm{BO}}T$ samples of input-output data are obtained in this procedure, all of which are used for system identification.

The frequency constraint introduced in Oshima et al. (2024) is also used to suppress the difference between the qualities of the $T$-sample data in the experiment of each iteration and the overall $N_{\mathrm{BO}}T$-sample data. Therefore, the optimization problem to be solved is

$$\max_{\boldsymbol{\chi}} J \tag{15}$$

subject to

$$\frac{\int_0^{T^{-1}} \Psi_{r_i}(\omega)\mathrm{d}\omega}{\int_{T^{-1}}^{1} \Psi_{r_i}(\omega)\mathrm{d}\omega} < \epsilon, \ \forall i \in \mathbb{Z}_{1\le,\le I}, \tag{16}$$

where $\{r_i\}$ is an external excitation signal, and $\Psi_{r_i}(\omega)$ is the power spectral density of $r_i$ for frequency $\omega \in (0, 1)$.

## 5. NUMERICAL EXAMPLE

The nonasymptotic E-optimal DoE is compared with the asymptotic E-optimal DoE in a numerical example. The hyperparameters $R$ and $\tilde{R}$ in the nonasymptotic DoE were set to 500 and 25, respectively. To clarify the difference between the nonasymptotic and asymptotic objective functions, all the details except for the DoE objective function are the same in both DoE methods.

The system of interest is an open-loop, 2-input, 3-output ARX system represented by

Table 1. Initial evaluation points in BO

| Iteration | $T_1$ | $T_2$ |
|---|---|---|
| 1 | 2.01 | 2.01 |
| 2 | 2.01 | 50 |
| 3 | 50 | 2.01 |
| 4 | 50 | 50 |
| 5 | 26.05 | 26.05 |

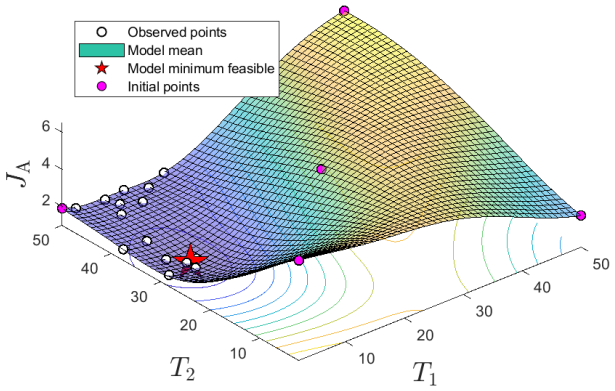


Fig. 1. Objective function of the asymptotic E-optimal DoE as a function of the design variables.

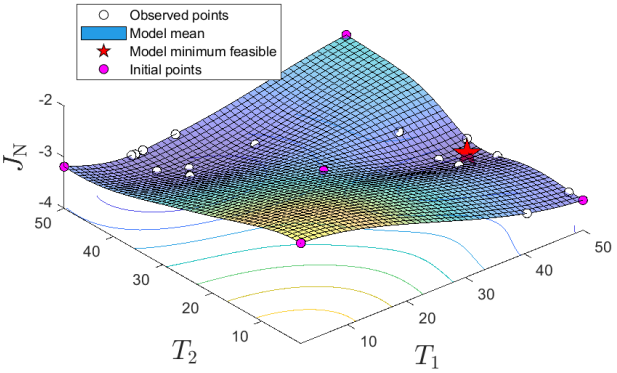


Fig. 2. Objective function of the nonasymptotic E-optimal DoE as a function of the design variables.

$$\boldsymbol{y}_t = \begin{bmatrix} 0.8535 & & 0 \\ & 0.9497 & \\ 0 & & 0.8475 \end{bmatrix} \boldsymbol{y}_{t-1} + \begin{bmatrix} 0.68 & 0.3033 \\ 0.2741 & 0.3014 \\ 0.1359 & 0.5248 \end{bmatrix} \boldsymbol{u}_{t-1} + \boldsymbol{e}_t, \tag{17}$$

where $\boldsymbol{e}_t \in \mathbb{R}^3$ follows an uniform distribution in $[-0.001, 0.001]^3$. Note that the seed values used to generate $\boldsymbol{e}_t$ are the same for both DoE methods. From Eq. (17), the system has three poles that take positive real values less than 1. This means the system is a stable process without oscillation, which is usual for process systems.

The input signals were

$$u_{m,t} = \sin\left(\frac{2\pi t}{T_m} + \frac{\pi}{2}(m-1)\right), \tag{18}$$

where $\{T_m\}$ are the period of the sinusoidal signal, and the design variables are $\boldsymbol{\chi} = [T_1, T_2]^\top$.

Table 2. The optimal design variables $T_1^*$, $T_2^*$, and the representative lengths $l_{\mathrm{SPS}}$ of nonasymptotic CRs for the asymptotic and nonasymptotic E-optimal DoE methods.

| DoE method | $T_1^*$ | $T_2^*$ | $l_{\mathrm{SPS}}\vert_{N_{\mathrm{BO}}T}$ |
|---|---|---|---|
| Asymptotic | 7.353 | 31.126 | $1.219 \times 10^{-4}$ |
| Nonasymptotic | 43.763 | 23.831 | $1.193 \times 10^{-4}$ |

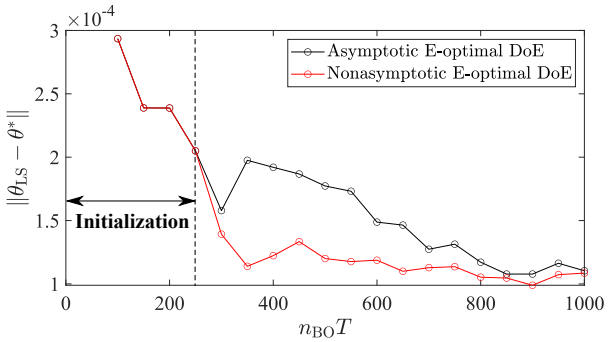


Fig. 3. The estimation error of the parameters for the nonasymptotic and asymptotic E-optimal DoE plotted as a function of the number of samples.

The maximum number of BO iterations $N_{\mathrm{BO}}$ was 20, and 50 samples were obtained in each iteration, that is, 1000 samples of input-output data were obtained. Since $T = 50$, Eq. (16) determines the upper limits of $T_m$ as 50. On the other hand, the lower limits of $T_m$ should be larger than 2 from the Nyquist sampling theorem. Hence, the optimal $\boldsymbol{\chi} \in \mathbb{R}^2$ was searched in $[2.01, 50]^2$ in this numerical example. Moreover, the first five iterations of BO were used to obtain the initial Gaussian process regression (GPR) model in BO, that is, $N_{\mathrm{BO,init}} = 5$. The design variables for the initial five experiments were set to the values in Table 1.

The GPR models of both objective functions were trained through DoE as shown in Figs. 1 and 2, respectively. The model mean fits well with the observed points in both figures, and hence, the GPR models for $J_{\mathrm{N}}$ and $J_{\mathrm{A}}$ are sufficiently accurate to be compared with each other.

The two GPR models are clearly different. Although the model of the asymptotic method has a single extremum, the model of the nonasymptotic method has two extrema. Moreover, the models of the nonasymptotic and asymptotic methods provide the optimal design variables $[T_1^*, T_2^*]^\top$ as shown in Table 2.

The least-squares estimate vectors of the nonasymptotic and asymptotic methods are also different. Calculation of $\boldsymbol{\theta}_{\mathrm{LS}}$ was performed to evaluate model accuracy, and $\|\boldsymbol{\theta}_{\mathrm{LS}} - \boldsymbol{\theta}^*\|$ is plotted as a function of $n_{\mathrm{BO}}T$ ($n_{\mathrm{BO}} \in \mathbb{Z}_{2\leq,\leq N_{\mathrm{BO}}}$) in Fig. 3. From Fig. 3, the nonasymptotic method provides the more accurate $\boldsymbol{\theta}_{\mathrm{LS}}$. Furthermore, the value of $l_{\mathrm{SPS}}$ at $n_{\mathrm{BO}}T = 1000$ was smaller in the nonasymptotic method as shown in Table 2. Hence, the nonasymptotic E-optimal objective function improves the performance of system identification.

## 6. CONCLUSIONS

A new DoE method using a data-quality index based on the maximum distance between the points in the nonasymptotic CR and the center of the nonasymptotic CR is proposed. In the proposed DoE, the nonasymptotic CR is calculated using the SPS method. Moreover, to effectively calculate the maximum distance for the proposed data-quality index, the proof of a theorem regarding the points on the boundary of the nonasymptotic CR is provided. The proposed DoE problem is solved in the same way as in Oshima et al. (2024).

The proposed DoE was compared with the asymptotic E-optimal DoE, which relies on the length of the longest axis of the asymptotic confidence ellipsoid, in a numerical example. As a result, the proposed DoE provided less least-squares-estimation error by 42.3% at the most.

However, the proposed method still has some open questions that will be answered in our future work. When the proposed method is used, a few hyperparameters, such as $T$ and $R$, need to be determined, which affects the performance of the proposed DoE. Although the effect of $T$ and $R$ on $\mathbb{D}_{\mathrm{SPS}}$ was studied by Csáji et al. (2015) and Weyer et al. (2017), how the changes in $T$ and $R$ affect the performance of the proposed DoE is not clear. A reasonable guideline to determine $T$ and $R$ should be derived so that the best performance of the proposed DoE can be obtained.

Another question is related to the accuracy of $l_{\mathrm{SPS}}$. The representative length $l_{\mathrm{SPS}}$ of $\mathbb{D}_{\mathrm{SPS}}$ is expressed using the $\boldsymbol{\theta}_{\max}$ calculated in Algorithm 1. The vector $\boldsymbol{\theta}_{\max}$ satisfies the necessary condition to be on a boundary of $\mathbb{D}_{\mathrm{SPS}}$ given in Theorem 1. However, it is not guaranteed that $\boldsymbol{\theta}_{\max}$ is the furthest point from $\boldsymbol{\theta}_{\mathrm{LS}}$ in $\mathbb{D}_{\mathrm{SPS}}$, and hence, $l_{\mathrm{SPS}}$ may be inaccurate. Although this risk is mitigated by decreasing $\delta l$ and increasing $I$, such adjustments of $\delta l$ and $I$ increase the computational cost. Hence, the relationship between them should be studied in detail to find a set of reasonable parameters balancing the computational cost and the accuracy of $l_{\mathrm{SPS}}$.

## ACKNOWLEDGEMENTS

M. O. was supported by a graduate exchange fellowship from JGP, Kyoto University.

## REFERENCES

Csáji, B.C., Campi, M.C., and Weyer, E. (2012). Sign-perturbed sums (SPS): A method for constructing exact finite-sample confidence regions for general linear systems. *Proceedings of the IEEE Conference on Decision and Control*, 7321–7326.

Csáji, B.C., Campi, M.C., and Weyer, E. (2015). Sign-perturbed sums: A new system identification approach for constructing exact non-asymptotic confidence regions in linear regression models. *IEEE Transactions on Signal Processing*, 63(1), 169–181.

Csáji, B.C. and Weyer, E. (2015). Closed-loop applicability of the sign-perturbed sums method. *54th IEEE Conference on Decision and Control (CDC)*, 1441–1446.

Franceschini, G. and Macchietto, S. (2008). Model-based design of experiments for parameter precision: State of

the art. *Chemical Engineering Science*, 63(19), 4846–4872.

Goodwin, G.C. (1977). *Dynamic system identification: experiment design and data analysis*, volume 136. Academic Press.

Kocis, L. and Whiten, W.J. (1997). Computational investigations of low-discrepancy sequences. *ACM Trans. Math. Softw.*, 23(2), 266–294.

Kolumbán, S. and Csáji, B.C. (2018). Towards d-optimal input design for finite-sample system identification. *18th IFAC Symposium on System Identification SYSID 2018*, 51(15), 215–220.

Ljung, L. (1998). *System Identification: Theory for the User*. Pearson, 2nd edition.

Morari, M. and H. Lee, J. (1999). Model predictive control: past, present and future. *Computers & Chemical Engineering*, 23(4), 667–682.

Oshima, M., Kim, S., Shardt, Y.A.W., and Sotowa, K.I. (2023). Extension of sign-perturbed sums method to multivariate systems. In *FOCAPO/CPC 2023*.

Oshima, M., Kim, S., Shardt, Y.A., and Sotowa, K.I. (2024). Experiment design taking nonasymptotic properties of the model into consideration. *IFAC-PapersOnLine*, 58(15), 550–555.

Shahriari, B., Swersky, K., Wang, Z., Adams, R.P., and de Freitas, N. (2016). Taking the human out of the loop: A review of bayesian optimization. *Proceedings of the IEEE*, 104(1), 148–175.

Shardt, Y.A.W. (2022). *Statistics for Chemical and Process Engineers-A Modern Approach*. Springer Cham.

Szentpéteri, S. and Csáji, B.C. (2023). Non-asymptotic state-space identification of closed-loop stochastic linear systems using instrumental variables. *Systems & Control Letters*, 178, 105565.

Weyer, E., Campi, M.C., and Csáji, B.C. (2017). Asymptotic properties of sps confidence regions. *Automatica*, 82, 287–294.

## Appendix A. PROCEDURE FOR THE SPS METHOD

The procedure for the SPS method is:

S.1 Determine $R \in \mathbb{Z}_{2\leq}$ and $\tilde{R} \in \mathbb{Z}_{1\leq,\leq R-1}$.

S.2 Generate $(R-1)$ time series of random-sign matrices $\{\boldsymbol{\Xi}_{1,t}\}_{t=1}^{T}, \cdots, \{\boldsymbol{\Xi}_{R-1,t}\}_{t=1}^{T}$. The random-sign matrix $\boldsymbol{\Xi}_{r,t} \in \mathbb{R}^{N\times N}$ is a diagonal matrix, whose diagonal components take the values $+1$ and $-1$ with a probability of 0.5 each.

S.3 Determine $\mathbb{D}_{\text{SPS}}$ using the following equation:

$$\mathbb{D}_{\text{SPS}} = \left\{ \boldsymbol{\theta} \in \mathbb{R}^d \mid \text{Rank}(\boldsymbol{\theta}) \leq R - \tilde{R} \right\}, \tag{A.1}$$

where $\text{Rank}(\boldsymbol{\theta})$ is calculated as follows:

S.3.1 Calculate $\{\boldsymbol{\epsilon}_{0,t}(\boldsymbol{\theta})\}_{t=1}^{T}$ defined as

$$\boldsymbol{\epsilon}_{0,t}(\boldsymbol{\theta}) = \boldsymbol{y}_t - \boldsymbol{\Phi}_t^{\top}\boldsymbol{\theta} \in \mathbb{R}^N \tag{A.2}$$

using the input-output data $\mathbb{S}_{\text{Data},0}$.

S.3.2 Calculate $\{\boldsymbol{\epsilon}_{1,t}(\boldsymbol{\theta})\}_{t=1}^{T}, \cdots, \{\boldsymbol{\epsilon}_{R-1,t}(\boldsymbol{\theta})\}_{t=1}^{T}$ as

$$\boldsymbol{\epsilon}_{r,t}(\boldsymbol{\theta}) = \boldsymbol{\Xi}_{r,t}\boldsymbol{\epsilon}_{0,t}(\boldsymbol{\theta}). \tag{A.3}$$

S.3.3 Generate the input-output data $\mathbb{S}_{\text{Data},r}(\boldsymbol{\theta})$ using the simulation of the system with $\boldsymbol{\theta}$ using $\boldsymbol{\epsilon}_{r,t}(\boldsymbol{\theta})$ as a noise innovation vector, for all $r \in \mathbb{Z}_{1\leq,\leq R-1}$. Note that the initial condition of the system for the simulation is the same as when the original data $\mathbb{S}_{\text{Data},0}$ is obtained.

S.3.4 Prepare $R$ regressor matrices $\{\boldsymbol{\Phi}_{\rho,t}\}_{\rho=0}^{R-1}$, where $\boldsymbol{\Phi}_{0,t} = \boldsymbol{\Phi}_t$, and $\boldsymbol{\Phi}_{r,t}$ $(r > 0)$ is composed of the data $\mathbb{S}_{\text{Data},r}(\boldsymbol{\theta})$ in the same way as $\boldsymbol{\Phi}_t$.

S.3.5 Calculate $\{\boldsymbol{s}_\rho(\boldsymbol{\theta})\}_{\rho=0}^{R-1}$ defined as

$$\boldsymbol{s}_\rho(\boldsymbol{\theta}) = \left(\frac{1}{T}\sum_{t=1}^{T}\boldsymbol{\Phi}_{\rho,t}\boldsymbol{\Phi}_{\rho,t}^{\top}\right)^{-\frac{1}{2}} \cdot \left(\frac{1}{T}\sum_{t=1}^{T}\boldsymbol{\Phi}_{\rho,t}\boldsymbol{\epsilon}_\rho(t,\boldsymbol{\theta})\right), \tag{A.4}$$

where $\boldsymbol{s}_0(\boldsymbol{\theta})$ and $\{\boldsymbol{s}_r(\boldsymbol{\theta})\}_{r=1}^{R-1}$ are the reference sum and the sign-perturbed sums, respectively.

S.3.6 Arrange $\{\|\boldsymbol{s}_\rho(\boldsymbol{\theta})\|\}_{\rho=0}^{R-1}$ from smallest to largest, and let $\|\boldsymbol{s}_{\rho_i}(\boldsymbol{\theta})\|$ be the $i$-th smallest.

S.3.7 Define $\text{Rank}(\boldsymbol{\theta})$ as

$$\text{Rank}(\boldsymbol{\theta}) = i, \text{ if and only if } \|\boldsymbol{s}_0(\boldsymbol{\theta})\| = \|\boldsymbol{s}_{\rho_i}(\boldsymbol{\theta})\|. \tag{A.5}$$

## Appendix B. PROOF OF THEOREM 1

Let us consider a parameter vector $\boldsymbol{\theta}_{\text{B}} \in \mathbb{B}_{\text{SPS}}$, then the points on a half line from $\boldsymbol{\theta}_{\text{LS}}$ to $\boldsymbol{\theta}_{\text{B}}$ are given as

$$\boldsymbol{\theta}(k) = k(\boldsymbol{\theta}_{\text{B}} - \boldsymbol{\theta}_{\text{LS}}) + \boldsymbol{\theta}_{\text{LS}}, \ k \geq 0. \tag{B.1}$$

Since $\boldsymbol{\theta}(1) = \boldsymbol{\theta}_{\text{B}}$ is a point on the boundary, Eq. (B.1) implies that, $\forall \boldsymbol{\theta}_{\text{B}} \in \mathbb{B}_{\text{SPS}}$, $\exists \overline{\Delta k} > 0$ s.t., $\forall \Delta k \in (0, \overline{\Delta k}]$,

$$\boldsymbol{\theta}(1 \pm \Delta k) \in \mathbb{D}_{\text{SPS}} \text{ and } \boldsymbol{\theta}(1 \mp \Delta k) \notin \mathbb{D}_{\text{SPS}}. \tag{B.2}$$

(double sign in the same order)

Furthermore, Eq. (B.2) is transformed as follows:

$$\begin{aligned}
\text{(B.2)} &\Leftrightarrow \begin{cases} \text{Rank}(\boldsymbol{\theta}(1 \pm k)) \leq R - \tilde{R} \\ \text{Rank}(\boldsymbol{\theta}(1 \mp k)) > R - \tilde{R} \end{cases} \quad (\because \text{From Eq. (6)}) \\
&\Leftrightarrow \begin{cases} \|\boldsymbol{s}_0(\boldsymbol{\theta}(1 \pm \Delta k))\| \leq \|\boldsymbol{s}_{\rho_{R-\tilde{R}}}(\boldsymbol{\theta}(1 \pm \Delta k))\| \\ \text{and} \\ \|\boldsymbol{s}_0(\boldsymbol{\theta}(1 \mp \Delta k))\| > \|\boldsymbol{s}_{\rho_{R-\tilde{R}}}(\boldsymbol{\theta}(1 \mp \Delta k))\| \end{cases} \\
&\quad (\because \text{From the definition of Rank}(\cdot) \text{ in Eq. (A.5)}) \\
&\Leftrightarrow f(1 \pm \Delta k) \leq 0 \text{ and } f(1 \mp \Delta k) > 0 \qquad \text{(B.3)}
\end{aligned}$$

(double sign in the same order)

where $f : \mathbb{R} \mapsto \mathbb{R}$ is a univariate and continuous function defined as $f(\cdot) = \|\boldsymbol{s}_0(\boldsymbol{\theta}(\cdot))\| - \|\boldsymbol{s}_{\rho_{R-\tilde{R}}}(\boldsymbol{\theta}(\cdot))\|$. Thus, applying the intermediate value theorem to Eq. (B.3) gives

$$\exists k' \in [1 - \Delta k, 1 + \Delta k] \text{ s.t. } f(k') = 0. \tag{B.4}$$

Since $f(k') = 0$ is equivalent to

$$\|\boldsymbol{s}_0(\boldsymbol{\theta}(k'))\| = \|\boldsymbol{s}_{\rho_{R-\tilde{R}}}(\boldsymbol{\theta}(k'))\|, \tag{B.5}$$

that is, $\text{Rank}(\boldsymbol{\theta}(k')) = R - \tilde{R}$ (Csáji and Weyer, 2015), Eq.(B.4) is

$$\exists k' \in [1 - \Delta k, 1 + \Delta k] \text{ s.t. } \text{Rank}(\boldsymbol{\theta}(k')) = R - \tilde{R}. \tag{B.6}$$

Eq. (B.6) holds for all $\Delta k \in (0, \overline{\Delta k}]$. Let us consider the limit as $\Delta k$ goes to 0, then the set $[1-\Delta k, 1+\Delta k]$ converges to $\{1\}$. Therefore, Eq. (B.6) implies

$$\text{Rank}(\boldsymbol{\theta}(1)) = R - \tilde{R}. \tag{B.7}$$

Since $\boldsymbol{\theta}(1) = \boldsymbol{\theta}_{\text{B}}$ from Eq. (B.1), Eq. (B.7) is

$$\text{Rank}(\boldsymbol{\theta}_{\text{B}}) = R - \tilde{R}. \tag{B.8}$$

Thus, the rank function returns $R - \tilde{R}$ for any point on the boundaries of the CR obtained using the SPS method. *Q.E.D.*